RSC Advances

ROYAL SOCIETY OF CHEMISTRY

www.rsc.org/advances

Journal Name

COMMUNICATION

Mesoporous Nano- WO_x/ZrO_2: Facile Synthesis and Improved catalysis

Received 00th January 20xx,
Accepted 00th January 20xx

DOI: 10.1039/x0xx00000x

www.rsc.org/

JunHua Zhu,[a,b] Kangjian Tang,[a,b,*] Yingchun Ye,[b] Xiaohong Yuan,[b] Weimin Yang[b,*] *and* Yi Tang[b]

A facile synthetic method was developed to prepare mesoporous nano- WO_x/ZrO_2 (MN-WZ). TEM, XRD, BET, UV-Vis, Raman and catalytic test were performed to investigate its mesoporous structure and acidity. Due to the abundant pores and corresponding permeability, the MN-WZ showed much improved catalytic performance on the conversion of n-pentane isomerisation.

Solid acid catalysts played an important role in a great number of petroleum and chemical processes,[1,2] such as catalytic cracking,[3] isomerization,[4,5] alkylation,[6] hydration and dehydration,[7] because of their high activity, convenient separation, lesser corrosion of reactors. Tungsten oxide-based materials such as WO_3/Al_2O_3,[8,9] WO_3/TiO_2,[10,11] WO_3/SiO_2,[12,13] and WO_3/ZrO_2,[14-18] are considered promising solid acid catalysts, owing to their strong acidity and thereby notable activity for various catalytic reactions, especially the strongest one, WO_3/ZrO_2. In our previous work,[19,20] we made a series of nanosized WO_x/ZrO_2 catalysts via a two-phase interface hydrolysis (TPIH) method, whose aim was to improve its dispersion threshold and to make more effective acid sites. Results showed that nano- WO_x/ZrO_2 had higher dispersion threshold (ca.0.372g WO_x/g ZrO_2 and 6.2 W atoms/nm^2) and increased one time conversion rate than conventional ones on the catalytic reaction of n-pentane isomerisation. However, a serious problem, fast inactivation by coke, then followed. Actually, porous materials with macropore, mesopore or micropore can provide a high surface area and better permeability.[21-26] The better permeability would offer better coke-tolerance. This is to find one suitable method of preparing some porous nano- WOx/ZrO_2 catalysts and to solve the problem of fast inactivation on n-pentane isomerisation.

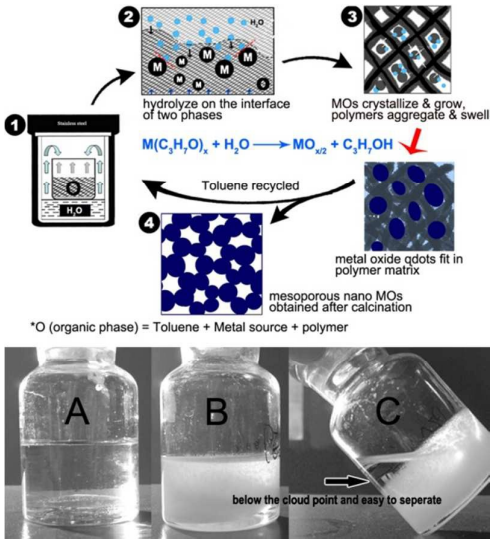

Scheme 1. Schematic diagram for the preparation process of mesoporous nano-WO_x/ZrO_2. M means metal alkyl oxide precursor.

This paper is aimed to develop some facile preparative method to fabricate porous nano- WO_x/ZrO_2 and extend to general preparation of nanocomposite. In this work, we developed a TPIH and polymer-template method to prepare mesoporous nano- WO_x/ZrO_2 (NM-WZ) and investigated its performance on the catalytic reaction of n-pentane isomerisation. Scheme 1 presents the process of preparation on NM-WZ by combining TPIH and polymer-template method. The water phase and the organic phase (e.g. toluene) were placed separately in a two-chambered Teflon-lined autoclave, and metal alkyl oxide precursors (M: $W(OC_3H_7)_6$ and $Zr(OC_3H_7)_4$) and polymer solution were added into the organic phase. Under the reacted temperatures over 100°C, the two phases evaporated and diffused within the autoclave and hydrolysis reaction occurred at their interface area. At the same time, metal oxides crystallized within the confined spaces of swelled polymer matrix and the nano-WO_x/ZrO_2/polymer formed. The gel-like monolith of obtained composite can be easily separated from the parent organic solvent due to the characteristic segregation of the polymer below cloud point[27] (as shown in A, B and C parts). The organic phase could be

[a] *Department of Chemistry, Fudan University, Shanghai 200433, (P.R. China) Fax: +86-21-65641740; Tel: +86-21-55664125*
[b] *Shanghai Research Institute of Petrochemical Technology, SINOPEC, Shanghai, 201208 (P. R. China). Fax: +86-21-68462283; Tel: +86-21-68462197-1202; E-mail: tangkj.sshy@sinopec.com & yangwm.sshy@sinopec.com*
[c] *Footnotes relating to the title and/or authors should appear here.*
Electronic Supplementary Information (ESI) available: [details of any supplementary information available should be included here]. See DOI: 10.1039/x0xx00000x

recycled for the next round reaction and MN-WZ was obtained after direct calcination under 650°C.

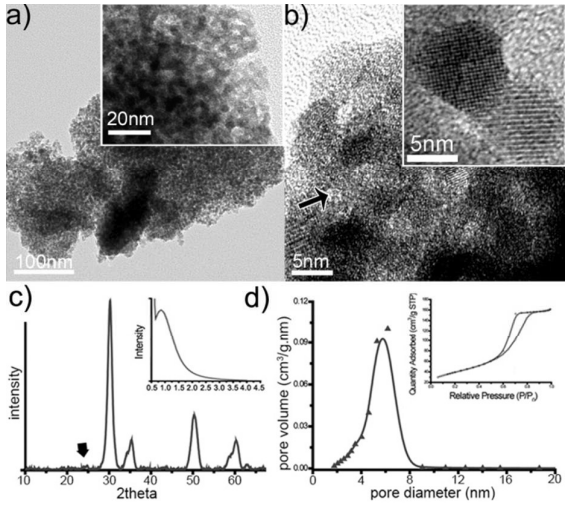

Fig .1 a) low resolution and b) corresponding high resolution TEM images of MN-WZ, the arrow indicates the pore with diameter of around 5nm. (inset: further magnified image show the detailed observation of heterojunction between tetragnol-ZrO_2 and WO_3). c) XRD pattens, (inset: diffraction at small angle) and d) curve of pore distribution. (Inset: curve of N_2 adsorption/desorption)

Figure 1a is the typical transmission electron microscope (TEM) image for MN-WZ prepared at thermal temperature of 150°C and calcined at 650°C for 12h, which shows the product has abundant porous structures. The corresponding high-resolution TEM image (inset, Figure 1a) shows that the pores, formed by the stack of nanoparticles. It appears to be interconnected and have wormlike shape. The determinate components of W-O-Zr are detected by energy dispersive (EDX) method (see supporting information Figure. S1). Figure 1b shows the amplified mesoporous structure and observed crystal lattices. The inset shows one interesting observation of a heterojunction between WO_3 and ZrO_2. Powder X-ray diffraction (XRD) measurement and N_2 adsorption/ desorption were carried out to investigate the characterizations of as-prepared MN-WZ. The characteristic peaks of t-ZrO_2 can be found completely in the XRD patterns as seen in figure 1c. The broad peaks imply the ZrO_2 are very small nanoparticles, which is in agreement with the observation from HRTEM. At the same time, the typical diffraction of m-ZrO_2 and m-WO_3 couldn't be detected, which implies the WO_x are highly dispersed on the surface of t-ZrO_2. The broad peak at the small-angle range from 0.6°~1.5° shows the mesopores have a wide distribution of porous diameter. Figure 1d is the curve of distribution of porous diameter based on nitrogen adsorption/desorption, which shows the products possess around 6nm of diameter and rich mesopores. This result is in agreement with the observation of HRTEM, as well. The BET surface is calculated to 160m^2/g，which is 6 times higher than WO_x/ZrO_2 obtained by impregnated method.[28]

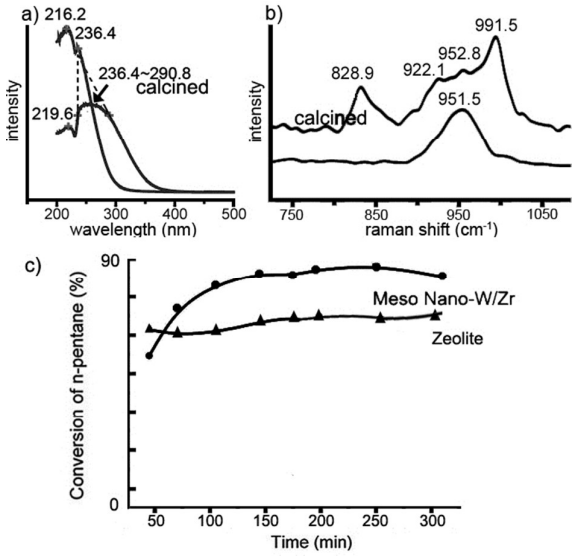

Fig .2 a) UV-Vis absorption and b) Raman spectrum of as-prepared MN-WZ. c) The conversion of cymene hydroperoxide. (●) MN-WZ with W-O-Zr strong interaction, (calcined under 650 °C) and (▲) referenced zeolite MCM-22 catalyst.

The MN-WZ was further evaluated by UV-Vis, Raman spectra and a fast catalytic test toward to acidity. As seen in figure 2a, the nano-WO_x-ZrO_2 without calcinations has two absorption peaks, 216.2 nm and 236.4 nm, which could be affiliated to the inherent absorption of nano ZrO_2 and WO_x, respectively. After thermal treatment at 650 °C for 8 h, the absorption peak locating at 216.2 nm changed to 219.6 nm, which corresponded to the slight growth of nano-ZrO_2; and that locating at 236.4 changed to a broaden absorption from 236.4 nm to 290.8 nm, which corresponded to the electron transition through the heterojunction between WO_x and ZrO_2 and a variety of WO_x states. Figure 2b shows the Raman spectrum with the range from 720 cm^{-1} to 1080 cm^{-1}. It can be seen that the sample before calcination just has one broad absorption peak, indicating the stretching modes of W-O or W-O-W (~951.5cm^{-1}) from a variety of tungstate species.[29] Then four peaks appeared after calcinations, which could be attributed to stretching modes of W-O-W (~828.9 cm^{-1}, from WO_3), W-O-W or W-O (922.1 cm^{-1} and 952.8 cm^{-1}, from two tungstate species), W=O oxo group (~991.5 cm^{-1} and 1020 cm^{-1}, from small oligomeric clusters). Figure 2c shows the compared catalytic result on the reaction from cymene hydroperoxide (CHP) to phenol and acetone.[30,31] The referenced catalyst is zeolite MCM-22, which is one traditional industrial catalyst. It can be seen that, for MN-WZ, the conversion rate after 20 minutes was 53.6%, then rapidly increased to 86.1% after 120 minutes and kept almost unchanged. The referenced zeolite showed the conversion rate was alwayls arount 75%. The compared result revealed that our MN-WZ catalyst have a higher catalytic efficiency than referenced zeolite. These three results all implied that the MN-WZ has strong acidicity, which was from the interaction between W-O-Zr. That's to say, the polymer induced is simply one pore-template and there is no negtive affection on the WO_x/ZrO_2 materials.

To solve previous problem, as-prepared MN-WZ catalysts were tested preliminarily on conversion of n-pentane. Figure. 3 shows the compared catalytic results based on MN-WZ and

TPIH-WZ. The TPIH-WZ lost its activity as quickly as reported previously.[19b] But the MN-WZ kept its activity aroud 22% and stabilized. This MN-WZ catalysts offered more improved catalysis on n-pentane isomerisation

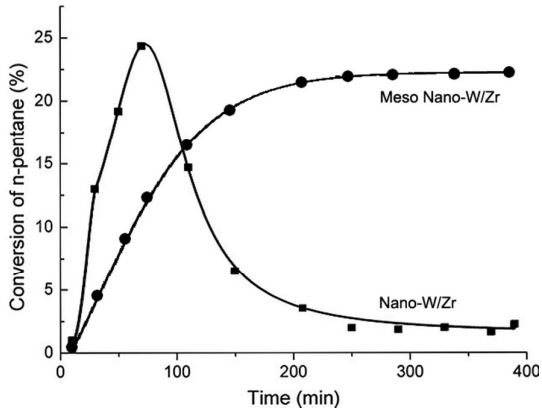

Fig .3 Compared conversion of n-pentane catalyzed by MN-WZ and TPIH-WZ (ref.) at 523 K with WHSV of 2.25 h^{-1}.

As reported, working on the investigation of WO_x state on ZrO_2 is always an important work,[32,33] but the nature of the interaction between WO_x and ZrO_2 was still uncertain. Inspired by the observation of the heterojunction in HRTEM (figure 2b), we tried to build a relationship between W and Zr, which may help to understand the nature of WO_x on ZrO_2. The patterns of (001) crystal face tailored from simulated t-ZrO_2 (figure 4a) and m-WO_3 (figure 4c) are matched to the structures viewed on TEM images. Then the connected faces were located to the faces of t-ZrO_2 (110) (figure 4b) and m-WO_3 (010) (figure 4d). It could be seen that one corner Zr atom connected two four-coordinated oxygen atoms, and total eight four-coordinated oxygen atoms connected one central Zr atom. Eight bonds from four four-coordinated oxygen atoms were used to connect W atoms. Similarly, six-coordinated W atoms interlacedly connect each other *via* two-coordinated oxygen. Eight bonds from eight two-coordinated oxygen atoms were used to connect Zr atoms. As measured, a certain distance of W-W is 0.499nm, which is much close to the distance of opposite Zr-Zr in one plane (0.515nm). The distance might be the reason why m-WO_3 connected t-ZrO_2 with inclined edge. Herein, the refined structure, (four 0.25Zr + one 1.0Zr atoms and four 0.25W atoms connect oxygen to compose the WO_x/ZrO_2, the final molar ratio of Zr to W is 2 to 1) could be drawn as a speculation, which is well accordant to the structure of WO_x/ZrO_2 as ensured.[34,35]

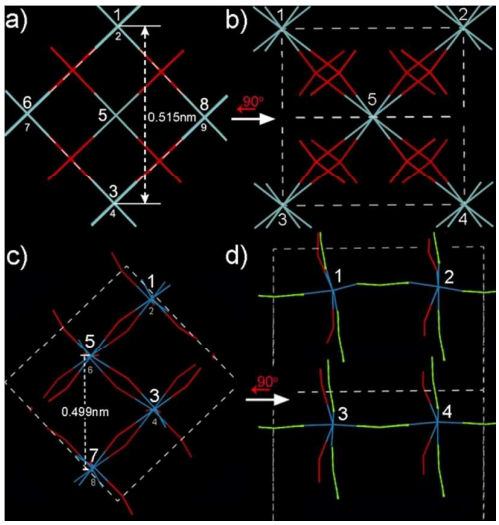

Fig .4 a) View of ZrO_2 (001) face (1, 3, 6, 8 atoms at front layer and 2, 4, 7, 9 atoms at back layer), b) ZrO_2 (110) face after turning 90° from (001) face; c) View of WO_3 (001) face (1, 3, 5, 7 atoms at front layer and 2, 4, 6, 8 at back layer), d) WO_3 (010) face after turning 90° from (001).

Conclusions

In conclusion, a facile synthetic method is described to prepare mesoporous nano WO_x/ZrO_2 *via* a polymer confined two-phase hydrolysis reaction under thermal condition. The essence of our method is the combination of the interface hydrolysis and nano-confined nucleation process in the polymer matrix, through which the wall thickness (particle size) and pore size (removing of the polymer) could be adjusted easily. With the abundant pore structure and permeability, on the preliminary test of the n-pentane conversion, the prepared mesoporous nano- WO_x/ZrO_2 showed much improved catalytic performance. We think that, the method is general to easily prepare porous nanocomposites and the recycling of solvent make environment friendly and a little low-cost.

Acknowledgements

The authors thank the financial support from the SINOPEC and National Natural Science Foundation of China (NSFC 21373272). The authors also thank Prof. Yahong Zhang for polishing our language.

Notes and references

† Electronic Supplementary Information (ESI) available: EDX patterns of as-prepared mesoporous WO_x/ZrO_2 nanocomposite. See DOI: 10.1039/b000000x/

Experimentals

1. In a typical synthesis, about 9 mL water was added into a Teflon lined stainless steel autoclave. Subsequently, 0.3 g zirconium isopropanol, 0.1 g tungsten isopropanol, and 0.3 g PEG were dissolved in 9 mL of toluene to serve as an organic phase. Then this solution was transferred into the inner container which was placed in a Teflon line above the surface of water. The autoclave was then sealed and placed in a preheated oven and heated statically at 150 °C for 24 h. After cooling down, the solid product was

separated by picking up the gel from solvent and calcined under 600 ^{o}C for 5 h.

2. The experiment of developing phenol and acetone from cymene hydroperoxide was carried out in a glass-flask with condensator. The as-prepared mesoporous nano-WO_x/ZrO_2 powders (0.2 g) were dispersed in a mixed solution with 10mL acetone, 8mL CHP/cymene (35 % CHP in cymene) and kept stirring. The reaction temperature was controlled at 80^{o}C. The conversion was measured about every 30 minutes. The amounts of acetone, cymene and cymene hydroperoxide evolved were analysized by gas chromatography. (Agilent GC-6820 TCD, Ar carrier).

3. Preliminary catalytic performance isomerization of n-pentane was evaluated in a down-flow fixed-bed reactor. 0.1 g of mesoporous nano-WO_x/ZrO_2 was placed in the central region of the reactor, with each end filled with quartz sand. Before the reaction, the catalyst was pretreated at 673 K under flowing dry air for 2 h to remove the adsorbed moisture. Then, the reactor was cooled to the reaction temperature under flowing high-purity nitrogen. The reactant n-pentane was pretreated by out-gassing and filtration and then introduced *via* a SSI Series II digital pump. The flow rate was 0.006 mL/min, corresponding to a WHSV of 2.25 h^{-1}. Then, the liquid n-pentane was gasified in an evaporation chamber at 473 K. After that, the gaseous n-pentane underwent an isomerization reaction in the fixed-bed reactor. The products were analyzed by online gas chromatography with a HP-alumina capillary column and a flame ionization detector (FID).

4. X-ray powder diffraction analysis of the products were carried out on a Bruker D8 X-ray diffractometer with CuKα radiation (λ = 1.5418 Å; 40 kV, 200 mA). The TEM and high resolution TEM analysis of the products were performed on FEI Tecnai 20 STWN. N_2 adsorption was measured on a Micromeritics Tristar 3000 instrument. The Raman property was investigated on a Dilor Labram–1B spectrometer and UV-vis property was investigated on a Varian cary-5000 spectrometer.

References

1. K. Tanabe, W.F. Holderich, Appl. Catal. A Gen. 1999, **181**, 399.
2. H. Hattori, Top. Catal., 2010, **53**, 432.
3. N. Rahimi, R. Karimzadeh, Appl. Catal. A Gen. 2011, **398,** 1.
4. V. Adeeva, H.Y. Liu, B.Q. Xu, W.M.H. Sachtler, Top. Catal. 1998, **6**, 61.
5. Y.D. Xia, W.M. Hua, Y. Tang, Z. Gao, Chem. Commun. 1999, 1899.
6. B.M. Reddy, M.K. Patil, Chem. Rev. 2000, **109**, 2185.
7. A. Micek-Ilnicka, J. Mol. Catal. A Chem. 2009, **308,** 1.
8. X.Y. Chen, G. Clet, K. Thomas, M. Houalla, J. Catal. 2010, **73**, 236.
9. V.M. Benitez, N.S. Figoli, Catal. Commun. 2002, **3**, 487.
10. H. Zhang, J. Han, X.W. Niu, X. Han, G.D. Wei, W. Han, J. Mol. Catal. A Chem. 2011, **350**, 35.
11. J. Engweiler, J. Harf, A. Baiker, J. Catal. 1996, **159**, 259.
12. A. Spamer, T.I. Dube, D.J. Moodley, C. van Schalkwyk, J.M. Botha, Appl. Catal. A Gen. 2003, **255**, 153.
13. C. van Schalkwyk, A. Spamer, D.J. Moodley, T. Dube, J. Reynhardt, J.M. Botha, Appl. Catal. A Gen. 2003, **255**, 121.
14. N. Soultanidis, W. Zhou, A.C. Psarras, A.J. Gonzalez, E.F. Iliopoulou, C.J. Kiely, I.E. Wachs, M.S. Wong, J. Am. Chem. Soc. 2010, **132**, 13462.
15. R.D. Wilson, D.G. Barton, C.D. Baertsch, E. Iglesia, J. Catal. 2000, **194**, 175.
16. I.E. Wachs, T. Kim, E.I. Ross, Catal. Today 2006, **116**, 162.
17. S. Kuba, P. Lukinskas, R.K. Grasselli, B.C. Gates, H. Knozinger, J. Catal. 2003, **216**, 353.
18. D.G. Barton, S.L. Soled, E. Iglesia, Top. Catal. 1998, **6**, 87.
19. K. Tang, J. Zhang, W. Yan, Z. Li, Y. Wang, W. Yang, Z. Xie, T. Sun, H. Fuchs, J. Am. Chem. Soc. 2008, **130**, 2676;
20. K. Song, H. Zhang, Y. Zhang, Y. Tang, K. Tang, J. Catal. 2013, **299**, 119.
21. C. T. Kresge, M. E. Leonowicz, W. J. Roth, J. C. Vartuli, J. S. Beck, Nature 1992, **359**, 710-713.
22. H. Meng, M. Xue, T. Xia, Z. Ji, D. Y. Tarn, J. I. Zink, A. E. Nel, ACS Nano, 2011, **5,** 4131.
23. M. S. Wong, E. S. Jeng, J. Y. Ying, Nano Lett., 2001, **11**, 637.
24. W. Wu, Z. Wang, W. Chen, M. Zhu, D. Zhang, Micro. Meso. Mater., 2015, **217**, 12-20.
25. R. Wei, H. Yang, D. Zhang, RSC. Adv. 2015, **5,** 63765–63776.
26. W. Wu, Z. Wan, M. Zhu, D. Zhang, Micro. Meso. Mater., 2016, 223, 203–212
27. J.S. Huang, M. W. Kim, Phys. Rev. Lett. 1981, **47**, 1462.
28. M. Hino, S. Kobayashi, K. Arata, Chem. Comm.1979, 6430.
29. M. Scheithauer, R. K. Grasselli, H. Knzinger, Langmuir 1998, **14**, 3019-3029.
30. A. Streitwieser, C. H. Heathcock, 1992. Introduction to Organic Chemistry. Kosower, E.M. (4th edition.). New York: MacMillan. 1018.
31. K. P. C. Vollhardt, N. E. Schore, 2003. Organic Chemistry: Structure and Function (4th edition.). New York: Freeman. 988.
32. M. Scheithauer, R. K. Grasselli, H. Knözinger, Langmuir, 1998, **14**, 3019.
33. D. G. Barton, M. Shtein, R. D. Wilson, S. L. Soled, E. Igelsia, J. Phys. Chem. B., 1999, **103**, 630.
34. J. A. Horsley, I. E. Wachs, J. M. Brown, G. H. Via, F. D. Hardcastle, J. Phys. Chem. 1987, **91**, 4014-4020.
35. F. Hilbrig, H. E. Gobel, H. Knözinger, H. Schmelz, B. Lengeler, J. Phys. Chem. 1991, **95**, 6973-6978.

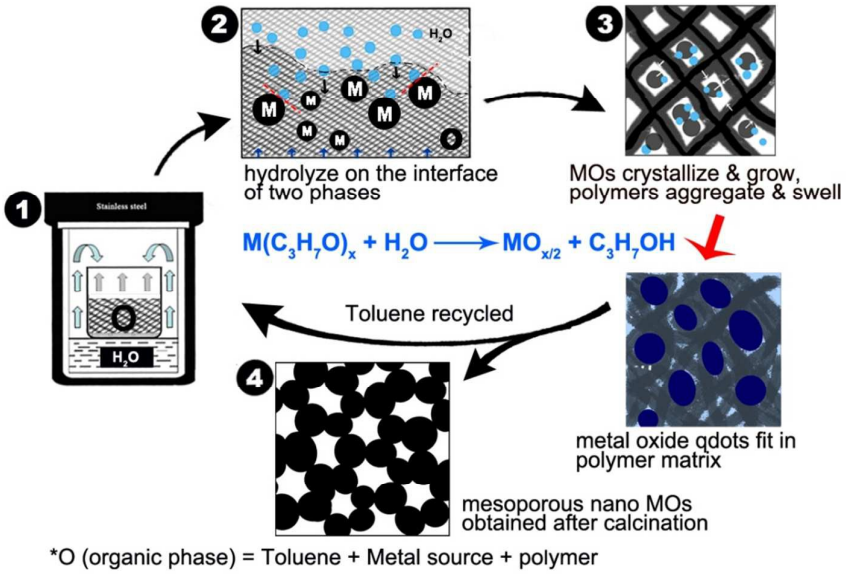

Schematic diagram for the preparation process of mesoporous nano-WO_x/ZrO_2.